Biochimica et Biophysica Acta 1854 (2015) 1906–1913

Contents lists available at ScienceDirect

Biochimica et Biophysica Acta

journal homepage: www.elsevier.com/locate/bbapap

A crystal structure of 2-hydroxybiphenyl 3-monooxygenase with bound substrate provides insights into the enzymatic mechanism

Margarita Kanteev [a,1], Almog Bregman-Cohen [a,1], Batel Deri [a], Anat Shahar [b], Noam Adir [c], Ayelet Fishman [a,*]

[a] Department of Biotechnology and Food Engineering, Technion-Israel Institute of Technology, Haifa, Israel
[b] Macromolecular Crystallography Research Center (MCRC), Department of Life Sciences & NIBN, Ben-Gurion University of the Negev, Beer-Sheva, Israel
[c] Schulich Faculty of Chemistry, Technion-Israel Institute of Technology, Haifa, Israel

ARTICLE INFO

Article history:
Received 13 April 2015
Received in revised form 6 August 2015
Accepted 9 August 2015
Available online 11 August 2015

Keywords:
2-Hydroxybiphenyl 3-monooxygenase (HbpA)
Flavin monooxygenases
2-Hydroxybiphenyl
Site-specific mutagenesis
Crystallography

ABSTRACT

2-Hydroxybiphenyl 3-monooxygenase (HbpA) is an FAD dependent monooxygenase which catalyzes the *ortho*-hydroxylation of a broad range of 2-substituted phenols in the presence of NADH and molecular oxygen. We have determined the structure of HbpA from the soil bacterium *Pseudomonas azelaica* HBP1 with bound 2-hydroxybiphenyl, as well as several variants, at a resolution of 2.3–2.5 Å to investigate structure function correlations of the enzyme. An observed hydrogen bond between 2-hydroxybiphenyl and His48 in the active site confirmed the previously suggested role of this residue in substrate deprotonation. The entrance to the active site was confirmed by generating variant G255F which exhibited only 7% of the wild-type's specific activity of product formation, suggesting inhibition of substrate entrance into the active site by the large aromatic residue. Residue Arg242 is suggested to facilitate FAD movement and reduction as was previously reported in studies on the homologous protein *para*-hydroxybenzoate hydroxylase. In addition, it is suggested that Trp225, which is located in the active site, facilitates proper substrate entrance into the binding pocket in contrast to aklavinone-11-hydroxylase and *para*-hydroxybenzoate hydroxylase in which a residue at a similar position is responsible for substrate deprotonation. Structure function correlations described in this work will aid in the design of variants with improved activity and altered selectivity for potential industrial applications.

1. Introduction

2-Hydroxybiphenyl 3-monooxygenase (HbpA) (EC 1.14.13.44) from the soil bacterium *Pseudomonas azelaica* HBP1, catalyzes the first step in the degradation of the fungicide 2-hydroxybiphenyl to 2,3-dihydroxybiphenyl (Fig. 1) [1]. HbpA was first discovered, purified and characterized by Kohler et al. [1,2]. It was shown that HbpA is an FAD dependent monooxygenase belonging to group A of flavin-dependent monooxygenases [3]. The enzyme catalyzes the *ortho* hydroxylation of a broad range of 2-substituted phenols in the presence of NADH and molecular oxygen [4–7].

Although flavin monooxygenases share low sequence identity, they all contain a common Rossmann fold responsible for FAD and/or NADH/NADPH binding [8–10]. The catalytic mechanism of flavin monooxygenases has been investigated through structural and kinetic studies [11]. Various studies on *para*-hydroxybenzoate hydroxylase (pHBH) and phenol hydroxylase (PH) have shown that the FAD cofactor changes its conformation during catalysis [12–18]. When FAD is situated in an "open" conformation, the isoalloxazine ring is exposed to the solvent region, enabling substrate entrance into the active site. Along with substrate binding, the isoalloxazine ring of FAD moves into the binding site, and adopts the "in" conformation. It was shown that in the active site of pHBH, the substrate undergoes deprotonation of the hydroxyl moiety through a hydrogen bond network [8,19]. The deprotonation step is essential for catalysis, since it increases the nucleophilic properties of the phenolic carbon to enable hydroxylation. In addition, it promotes FAD to adopt a third conformation, termed the "out" conformation, and interact with NADH for reduction. The reduced FAD moves into the binding site where it is oxidized by molecular oxygen, forming flavin C4a-hydroperoxide, a highly reactive intermediate which catalyzes the *ortho* hydroxylation of the substrate [9,20].

Several studies have shown that HbpA is able to catalyze the production of 3-substituted catechols, precursors for different pharmaceuticals [6,21]. In addition, directed evolution was used to generate variants with activity towards indole and its derivatives [22]. Furthermore, mutants with increased activity towards 2-*tert*-butylphenol and guaiacol were discovered highlighting residues which are important for activity and selectivity [6]. Since HbpA is a single-component enzyme, it was used as a model protein to study various methods for NADH regeneration, including enzymatic, chemical and electrochemical regeneration methods [5,23–26]. Recently, crystal structures of apo-HbpA and

Abbreviations: HbpA, 2-Hydroxybiphenyl 3-monooxygenase

* Corresponding author.
E-mail address: afishman@tx.technion.ac.il (A. Fishman).

[1] These authors equally contributed to the article.

http://dx.doi.org/10.1016/j.bbapap.2015.08.002
1570-9639/

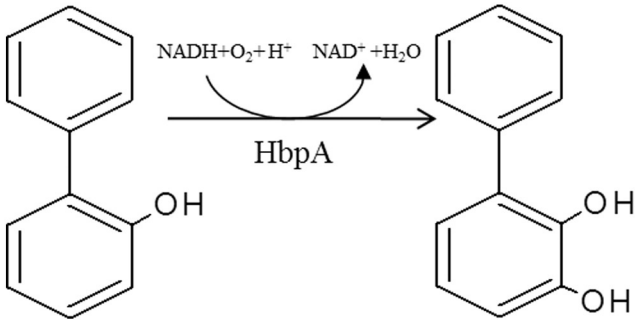

Fig. 1. The natural reaction catalyzed by 2-hydroxybiphenyl 3-monooxygenase (HbpA). 2-Hydroxybiphenyl is oxidized at the *ortho* position to form 2,3-dihydroxybiphenyl in the presence of oxygen and NADH.

HbpA with FAD bound in the "in" conformation were determined by Jensen et al., and it was found that residues His48, Asp117 and Arg242 play a role in catalysis [27].

In this study we determined the crystal structures of wild-type HbpA with 2-hydroxybiphenyl bound in the active site and several site specific variants at a resolution of 2.3–2.5 Å, in order to elucidate structure–function correlations and to expand and elaborate previous knowledge regarding the catalytic mechanism of HbpA.

2. Materials and methods

2.1. Reagents and materials

Methanol, acetonitrile, poly(ethylene glycol), kanamycin, imidazole, trizma base, 2,3-dihydroxybiphenyl, nicotinamide adenine dinucleotide (NADH) and flavin adenine dinucleotide (FAD) were purchased from Sigma-Aldrich Chemical Co. (Sigma-Aldrich, Rehovot, Israel). Trisodium citrate was purchased from J.T. Baker (Mallinckrodt Baker, Deventer, Holland). 2-Hydroxybiphenyl was purchased from Merck (Merck, Darmstadt, Germany).

2.2. Bacterial strains, plasmids and culture conditions

The sequence of the HbpA gene from *P. azelaica* HBP1 [1] was optimized for production in *Escherichia coli* (Optimum Gene™) and synthesized by Gen Script (Piscataway, NJ, USA) with addition of restriction sites of BamHI and NotI at the 5′-end and 3′-end respectively. The optimized gene was cloned into the pET9a (Novagen, Germany) and a His-tag was introduced to the N-terminus of the gene using primers listed in Supplementary Table S1. The vector pET9a/HbpA was transformed into *E. coli* BL21 (DE3; Novagen, Germany) for over-expression.

2.3. Expression and purification

E. coli cells harboring pET9a/HbpA were grown overnight at 37 °C in 0.5 l of TB medium with 25 μg ml^{-1} kanamycin, and harvested by centrifugation (8000× *g* for 10 min at room temperature). The cell pellet was re-suspended in a binding buffer (20 mM Tris-HCl buffer pH 7.5, 500 mM NaCl and 20 mM imidazole). The cells were broken using a homogenizer (EmulsiFlex-C3 High Pressure Homogenizer, Avestin, Ottawa, Canada) followed by centrifugation (16,000× *g* for 20 min at 10 °C) for the removal of cell debris. The supernatant was loaded onto a Ni(II)-bound affinity column which was initially equilibrated with the binding buffer. Fractions showing yellow color were eluted from the column with linear gradient of elution buffer (20 mM Tris–HCl buffer pH 7.5, 500 mM NaCl, and 500 mM imidazole) suggesting the presence of the FAD cofactor within the protein. In order to ensure complete protein loading with FAD, HbpA fractions were supplemented with additional FAD at a molar ratio of 1:1, incubated overnight and dialyzed against 20 mM Tris–HCl buffer, pH 7.5. The molecular mass of the purified HbpA was approximately 64 kDa as determined by SDS-PAGE, confirming previously reported results of Suske et al. [2].

2.4. Site-directed mutagenesis

HbpA variants R242A, R242E, R242Q, G255F, W225A and W225Y were created by Quick Change ®site-directed mutagenesis kit (Stratagene, CA, USA) as suggested by the manufacturer using the primers listed in Supplementary Table S1. Verification of the mutations was obtained by sequencing. Purification steps were identical to those performed on the wild type.

2.5. Expression and purification of Se-HbpA

The selenium–methionine labeling of HbpA (Se-HbpA) was prepared according to the protocol described by Lansky et al. [28]. Purification steps were identical to those performed on HbpA.

2.6. Analytical methods

The formation of 2,3-dihydroxybiphenyl and consumption of 2-hydroxybiphenyl was determined using high performance liquid chromatography (HPLC) with a Dionex UltiMate 3000 (Thermo Scientific) equipped with a Gemini 5 μ C18 110A column (5 μm, 4.6 × 250 mm; Phenomenex, Torrance, CA, USA), and the results were analyzed with Thermo Scientific Dionex Chromeleon software version 7.1 SRI. The isocratic elution was performed with acetonitrile: H_2O 40:60 (v/v). The reaction assay of 1 ml contained 50 mM phosphate buffer pH 7.5, 0.2 mM 2-hydroxybiphenyl, 0.15 μM protein and 0.4 mM NADH. Reactions of 30 min were stopped at different time points by the addition of 2 M HCl and diluted with methanol (0.5:1 v/v) prior to injection.

Steady state kinetics for 2-hydroxybiphenyl and NADH were measured by the decrease in absorption at 340 nm. All experiments were done in 50 mM phosphate buffer pH 7.5 with 1.55 μM protein. Kinetic parameters for 2-hydroxybiphenyl were determined in the presence of 0.4 mM NADH and 0.8–200 μM 2-hydroxybiphenyl, while kinetic parameters for NADH were determined with 0.2 mM 2-hydroxybiphenyl and 0.01–0.8 mM NADH. Endogenous NADH oxidation was determined by a control reaction without 2-hydroxybiphenyl and was used to correct NADH consumption. Kinetic constants were calculated using Graphite software. Each experiment was performed in 3–4 replicates.

2.7. Crystallization, data collection and structure determination

Crystallization trials were performed in 96 well hanging drop plates using MOSQUITO robot (TTP Labtech, Melbourne, UK) with a PEGs Suite (www.qiagen.com) at 20 °C. The crystals appeared after a week at a wide range of crystallization conditions which were further optimized. The optimal conditions contained 0.2 M sodium citrate and 25% PEG3350. The hanging drop contained 2 μl protein solution (6 mg ml^{-1}) and 2 μl crystallization condition. Soaking trials were performed as follow: 50 mM of 2-hydroxybiphenyl was added to the drop containing crystals, incubated overnight and then added again prior to freezing in liquid nitrogen [29]. X-ray diffraction data sets of Se-HbpA and HbpA_HBP were collected at the European Synchrotron Radiation Facility (ESRF), Grenoble, France, at beamlines ID14-4 and BM-14 respectively. X-ray diffraction data sets of wild type HbpA and variants W225Y, W225A and R242Q were collected in-house using X-ray beam R-Axis HTC (Rigaku, Japan). The diffraction data was indexed, integrated, and reduced with Mosflm and Scala [30] or with HKL2000 [31].

The first model of Se-HbpA was solved using a Phenix MR Rosetta Pipeline, and the model was further improved by AutoSol and AutoBuild [32]. After several cycles of phase improvements and model building, the obtained coordinates were used for molecular replacement using Phaser [33] to determine the high resolution structure of wild type HbpA. The structures of HbpA variants W225Y, W225A and R242Q

were solved using coordinates of wild type HbpA (HbpA-WT). Refinement was performed using Phenix [32]. Manual model building, real-space refinement, and structure validations were performed using Coot [34]. Crystal parameters and data statistics are summarized in Table S2 in the supplementary material.

2.8. Protein Data Bank accession numbers

Coordinates and structure factors of HbpA have been deposited in the RCSB Protein Data Bank under accession codes 4Z2R for HbpA-WT, 5BRT for HbpA_HBP, 4Z2T for W225Y and 4Z2U for R242Q (Table S2).

3. Results and discussion

3.1. Kinetic parameters of HbpA-WT

Kinetic studies of recombinant HbpA-WT were performed to determine the specific activity of NADH oxidation and product formation along with steady state kinetic parameters. In our study, the rate of product formation and NADH oxidation is about 2-fold lower than in previously reported studies (Table 1) [2,4]. However, the K_m value for 2-hydroxybiphenyl and the uncoupling percentage of NADH oxidation from product formation were found to be similar to the previously reported values, while the calculated k_{cat} value was about 6-fold lower (Table 2) [2,4,25]. We believe that these differences might be attributed to slightly different reaction conditions. The K_m value for NADH was calculated for the first time for HbpA at 30 °C, which is approximately the optimal temperature for its activity, and is about 10-fold lower than the respective values of recently published Baeyer-Villiger monooxygenases (Table 2) [7,35].

3.2. Structure determination

HbpA shares low sequence homology with other members of group A of flavin-dependent monooxygenases. In order to solve the phase problem, HbpA was labeled with selenium and a reliable model was obtained after numerous cycles of model building and phase improvements using Phenix MR Rosetta Pipeline, AutoSol and AutoBuild. This work was performed prior to the recent publication of the crystal structure of HbpA by Jensen and co-workers [27].

The structure of HbpA-WT was determined at a resolution of 2.3 Å using molecular replacement and coordinates of Se-HbpA. The crystal belongs to the monoclinic space group C2 with a dimer in the asymmetric unit. Although most of the protein regions as well as the FAD moiety were clearly defined with electron density above 2.4σ, two short flexible regions are missing in the protein structure due to the total lack of electron density (residues 228–238, 256–264). The overall structure of HbpA is similar to the recently published structures of Apo- and FAD-bound forms of HbpA (HbpA_apo and HbpA_IN, respectively) by Jensen et al., including the missing regions [27].

Table 1
Activity of engineered variants on NADH and 2,3-dihydroxybiphenyl.

Variant	Specific activity[a] (μmol min^{-1} mg protein^{-1})		Uncoupling[d] (%)
	Product formation[c]	NADH oxidation[b]	
WT	1.87	1.49	20
W225Y	2.35	1.82	23
W225A	0.25	0.11	60
R242A	0.10	NA[e]	–
R242E	0.12	NA	–
R242Q	0.23	NA	–
G255F	0.33	0.10	70

[a] The assays were performed at 30 °C in 50 mM phosphate buffer (pH 7.5) with 0.4 mM NADH and 0.2 mM 2-hydroxybiphenyl.
[b] Determined by monitoring NADH consumption at 340 nm. All values were corrected for the endogenous NADH oxidation and have a standard error of ≤10%.
[c] Determined by measuring substrate consumption and product formation with reverse phase HPLC.
[d] The percentage of uncoupling was calculated as the ratio of the NADH oxidation from the product formation.
[e] Not active.

3.3. The overall structure of HbpA

The monomer of HbpA can be subdivided into three domains, (i) the FAD binding domain (residues 1–77, 99–199, 294–436), (ii) the substrate binding domain (residues 78–98, 200–293) and (iii) the C-terminal domain (437–586) (Fig. 2). The FAD binding domain consists of a well-defined βαβ–Rossmann fold and a conserved motif of glycine residues GXGXXG (Fig. 4C) [36]. The substrate binding domain is found above the isoalloxazine ring of FAD and the C-terminal domain exhibits a classical thioredoxin fold [37]. However, in contrast to thioredoxin, the C-terminal domain does not contain a catalytic cysteine residue and thus has no thioredoxin activity. It seems that similar to aklavinone-11-hydroxylase (RdmE) and 3-hydroxybenzoate 4-hydroxylase (MHBH) the role of the HbpA C-terminal domain is to participate in quaternary structure formation [20,38].

3.4. Biological relevant unit

Suske et al. have previously reported that HbpA is a tetramer in solution with a molecular weight of 256 kDa [2]. The asymmetric content of the unit cell was analyzed using PISA (http://www.ebi.ac.uk/msd-srv/prot_int/pistart.html), and a tetrameric assembly was proposed with a buried surface of 16,300 Å^2 upon assembly formation. The tetramer has a sandwich like shape (Fig. 3A), built from two parallel disks, with each disk being composed from two protein molecules related by a crystallographic symmetry (Fig. 3B). These two protein molecules are positioned in a "head to tail" orientation, and polar interactions are formed between the C-terminal domain of one molecule and surface exposed residues of the neighboring molecule located on α17, β4 and β5 (Fig. 3D). Using a directed evolution approach to change substrate specificity of HbpA, Meyer et al. found that the replacement of Leu417 located on α17 (Fig. 2) to Phe, altered the catalytic properties of HbpA [4]. However, with the absence of an HbpA crystal structure, it was difficult to predict the influence of Leu417, distantly located from the active site, on enzyme activity. Having obtained a high resolution crystal structure of HbpA, we can now suggest that in contrast to Leu, which stabilizes the region via hydrophobic interactions with neighboring residues [27], Phe at position 417 may increase these interactions through π–π contacts with adjacent bulky hydrophobic residues such as Phe227, Tyr82 or Phe91 (Fig. 2). These three residues are located at the protein binding domain and interactions with Phe at position 417 might induce local conformational changes of the binding domain thus altering the catalytic properties of HbpA.

3.5. Structural homology to other flavin monooxygenases

Sequence analysis of HbpA, using NCBI Blast (http://blast.ncbi.nlm.nih.gov/Blast.cgi) revealed that HbpA shares low sequence homology with structurally characterized members of the flavin monooxygenase family such as pHBH, PH, MHBH, rebeccamycin biosynthetic enzyme (RebC) and RdmE, (below 33% identity), however the overall fold of the proteins is similar [12,15,20,38,39]. Structural comparison of HbpA with the homologous proteins mentioned above showed high similarity in their FAD binding domain and the C-terminal domain (except for pHBH). In contrast, the substrate binding domains and regions which participate in the quaternary structure formation exhibit strong variations among the different family members (Fig. S1).

Table 2
K_m and k_{cat} values of HbpA and engineered variants on 2-hydroxybiphenyl[a,b] and NADH.[a,c]

Variant	2-Hydroxybiphenyl			NADH		
	K_m (μM)	k_{cat} (sec^{-1})	k_{cat}/K_m (sec^{-1} μM^{-1})	K_m (μM)	k_{cat} (sec^{-1})	k_{cat}/K_m (sec^{-1} μM^{-1})
WT	3.1 ± 0.3	2.26	0.73	149 ± 22	3.16	0.02
W225Y	22.8 ± 3.3	4.51	0.2	102 ± 10	5.8	0.057
W225A	29.5 ± 3.5	0.46	0.02	253 ± 12	3.45	0.014
R242A	NC[d]	NC	NC	446 ± 57	0.14	3.14×10^{-4}
R242E	27.8 ± 2.2	0.15	5.4×10^{-3}	427 ± 107	0.15	3.51×10^{-4}
R242Q	NC	NC	NC	222 ± 34	0.24	1.08×10^{-3}
G255F	26.6 ± 2.9	0.71	0.03	531 ± 61	1.34	2.53×10^{-3}

[a] Determined by monitoring NADH consumption at 340 nm. All values were corrected for the endogenous NADH oxidation.
[b] The assays were performed at 30 °C in 50 mM phosphate buffer (pH 7.5) with 0.4 mM NADH and 0.0008–0.2 mM 2-hydroxybiphenyl.
[c] The assays were performed at 30 °C in 50 mM phosphate buffer (pH 7.5) with 0.2 mM 2-hydroxybiphenyl and 0.01–0.8 mM NADH.
[d] Not calculated. NADH consumption was very low and the effect of 2-hydroxybiphenyl concentration could not be examined. Therefore, K_m and k_{cat} were not calculated.

3.6. FAD binding domain

The FAD binding site forms an elongated, surface exposed pocket in the HbpA structure (Fig. 4A). The isoalloxazine ring of FAD is located between the FAD binding domain and the substrate binding domain and faces outside the binding pocket. This conformation of the isoalloxazine ring is known as the "out" conformation, while the "in" conformation of FAD was observed in the HbpA_IN structure determined by Jensen et al. [27]. The "out" conformation of isoalloxazine ring is stabilized in HbpA by structural water molecules and π–π interactions with Trp293, while in the "in" conformation, this Trp residue is flipped to protect the active site from the solvent (Fig. 4B) [15,27]. The "out" conformation of the isoalloxazine ring is also stabilized through polar interactions between Arg242 and the O4 of the FAD molecule (Fig. 4B and C). Interestingly, a similar orientation of Arg242 is observed in HbpA_apo despite the absence of FAD, but not in HbpA_IN. The distance between Arg242 and the O4 of the FAD molecule in the "in" conformation is about 7.2–7.3 Å. Apparently, the flexibility of Arg242 enables the conformational change of the FAD molecule, as was previously suggested (Fig. 4B) [13]. The ribityl moiety of FAD forms polar interactions with a conserved Arg46 residue. The phosphate moiety of FAD interacts with a conserved **GAGPAG** motif, GD motif, Arg46 and a conserved water molecule. Furthermore, the ribose moiety of ADP also interacts with the conserved **GAG**PA**G** motif (Fig. 4C) [36].

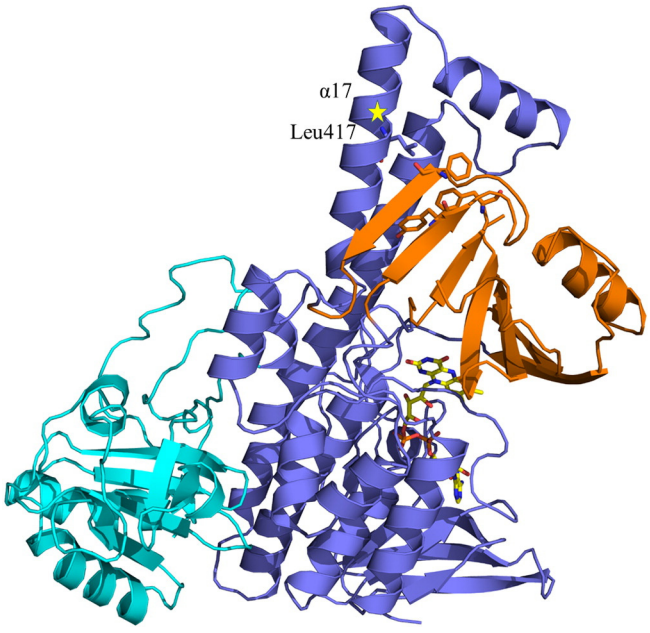

Fig. 2. The overall structure of HbpA monomer. Three main domains of HbpA are shown in the cartoon. The FAD binding domain is shown in blue, the substrate binding domain in orange and the C-terminal domain in cyan. The FAD molecule is shown in yellow sticks. Residue Leu417 which was found by Meyer et al. [4] to have an effect on protein activity is located on loop α17 and marked with a yellow asterisk. Hydrophobic residues at the close vicinity of Leu417 are shown as orange sticks.

3.7. Substrate entrance region

The substrate binding pocket of HbpA is located above the isoalloxazine ring of FAD and forms a contiguous tunnel to the protein exterior, revealing substrate entrance into the binding site. Similar to MHBH, this region is mostly composed of hydrophobic residues, which facilitate the entrance of a hydrophobic substrate [20]. The replacement of Gly255, located at the presumable substrate entrance site (Fig. 5A) to Phe, resulted in substantial decline in specific activity for both product formation and NADH oxidation (Table 1). While the efficiency (k_{cat}/K_m) of G255F for 2-hydroxybiphenyl is about 24-fold lower than HbpA-WT, its efficiency for NADH is only about 8-fold lower (Table 2). It seems that the replacement of Gly255 with Phe had a greater effect on product formation than on NADH oxidation, explaining the 70% uncoupling of NADH oxidation from product formation (Table 1). It is therefore suggested that a bulky Phe residue at position 255, limits substrate access to the binding site. As a result, G255F exhibited lower activity towards the substrate in comparison to the wild type enzyme, supporting our suggestion that indeed this region participates in substrate ingress. Nevertheless, it seems that Phe at position 255 affects also NADH oxidation. Since it is hard to predict which residues participate in NADH binding, it cannot be ruled out that position 255 participates in NADH binding or its oxidation.

3.8. Substrate binding domain

The substrate binding domain among the flavin-dependent monooxygenases is the most variable domain. This fact may be attributed to the diverse range of substrates which this group of enzymes oxidizes [10]. We succeeded in determining the crystal structure of HbpA with 2-hydroxybiphenyl in the active site of the enzyme (HbpA-HBP) at a resolution of 2.0–2.3 Å. In the HbpA-HBP structure, the FAD molecule is also found in the "out" conformation, similar to HbpA-WT. 2-Hydroxybiphenyl is located in the hydrophobic pocket of the active site, above the isoalloxazine ring of the FAD molecule and forms polar interaction with His48 (Fig. 6A). Previous studies by Jensen et al. have shown that the replacement of His48 with Ala abolished product formation and thus might be involved in substrate deprotonation [27]. The present work confirms this suggestion. It seems that similarly to Tyr201 in PHBH and His213 in 3-hydroxybenzoate 6-hydroxylase, where those residues activate the substrate for hydroxylation through a hydrogen bond with the hydroxyl of the substrate [40,12], in HbpA,

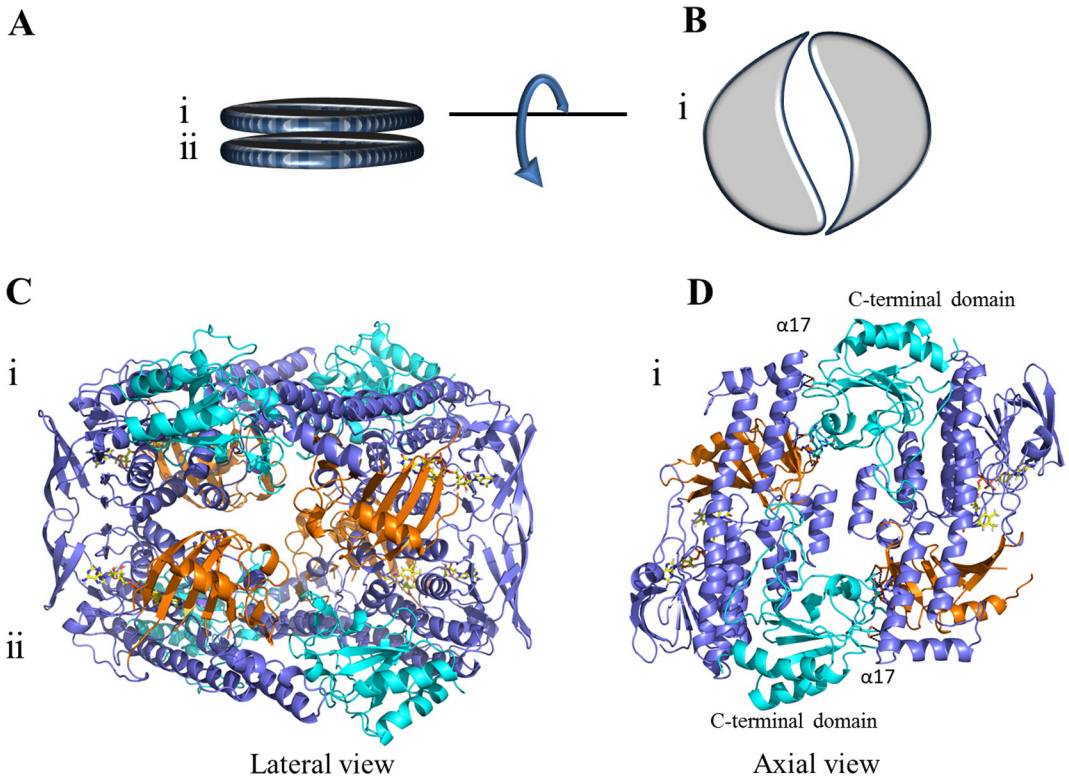

Fig. 3. Biologically-relevant unit composition of HbpA. A and B — Schematic presentation of the full tetramer (left) and by rotation a face presenting the dimer interactions (right). C and D — The lateral view of a tetrameric form of HbpA (left) and an axial form of a dimer (right) are shown in cartoon and colored similarly to Fig. 2.

this role is performed by His48. Interestingly, structural superposition of HbpA-HBP with HbpA_IN revealed that the *ortho* position of 2-hydroxybiphenyl is oriented above the C4 of the isoalloxazine ring, where molecular oxygen binds before hydroxylation occurs (Figs. 1 and 6B). In addition, it can be observed that 2-hydroxybiphenyl does not form any polar interactions except the interaction with His48;

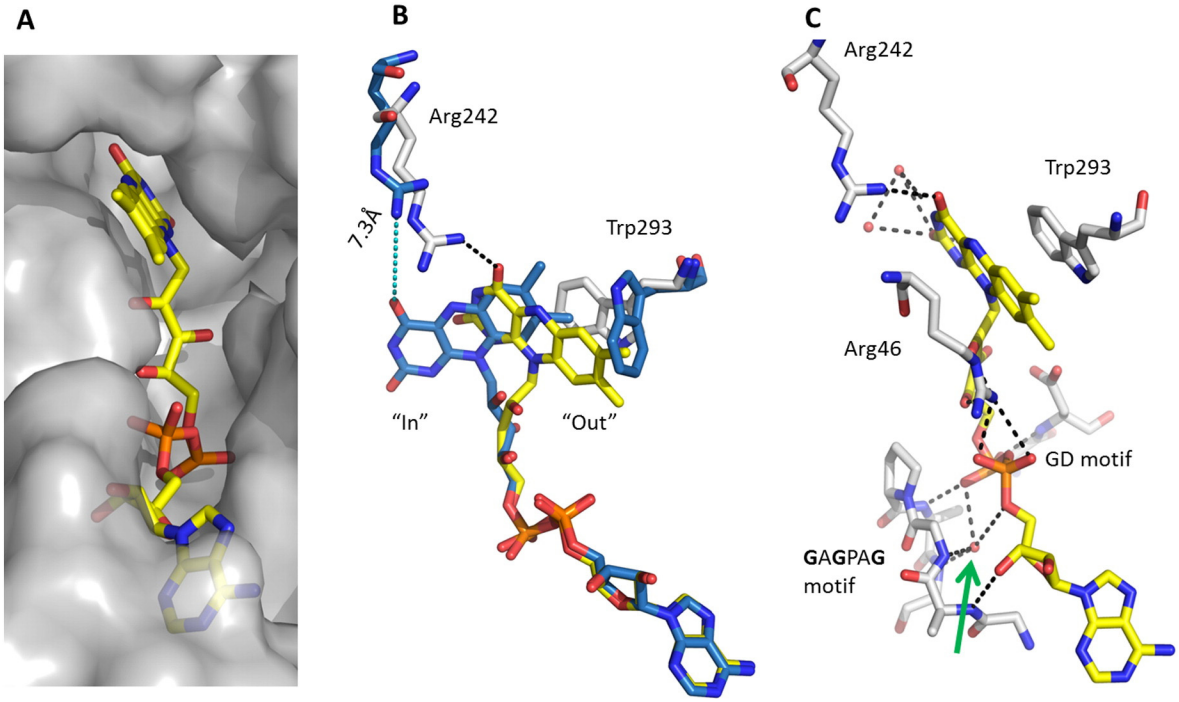

Fig. 4. FAD binding site. A. Surface presentation of the FAD binding cavity. B. The FAD binding domain of HbpA-WT (gray) is superimposed onto HbpA-IN (PDB code 4CY8, blue), the "out" conformation of FAD is shown in yellow and the "in" conformation in blue. A hydrogen bond between the FAD and Arg245 in HbpA-WT is shown as black dashed lines, while the distance between these objects in HbpA-IN is shown as cyan dashed lines. C. The extensive hydrogen bond interactions of FAD in the binding site. Hydrogen bonds are shown as black dashed lines and a conserved water molecule is shown as a red sphere and marked with a green arrow. For full explanations on interactions, see text.

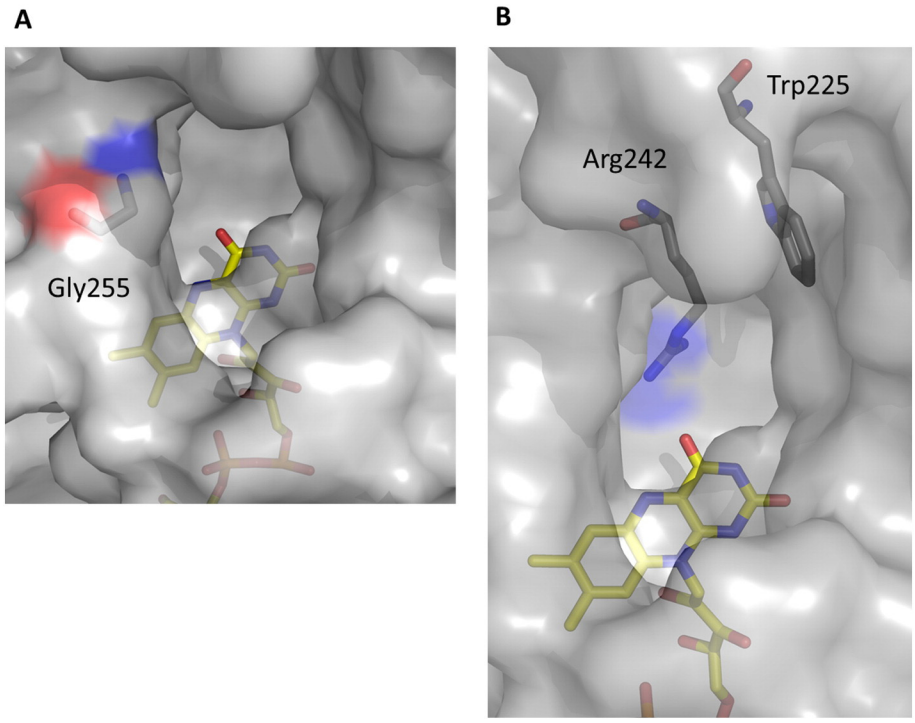

Fig. 5. Substrate entrance site. A. Surface presentation of a putative substrate entrance. The investigated Gly255 residue is shown in sticks. B. Surface presentation of substrate entrance and investigated residues Arg242 and Trp225 are shown as gray sticks.

moreover, almost all other residues in the active site are hydrophobic (Fig. 6A). Apparently, the unique architecture of the active site allows precise substrate orientation above the C4 of the isoalloxazine ring to enable hydroxylation. It seems that His48 is not only important for substrate deprotonation but also for substrate orientation in the active site. Jensen et al. reported that Asp117 is also important for hydroxylation, however, this residue does not form any interactions with the substrate (Fig. 6A). Apparently, as was proposed, the role of Asp117 is to stabilize the conformation of His48 to enable proper substrate orientation in the binding site [27]. In order to shed more light on the mechanism of HbpA, we focused on two residues, located at the substrate binding pocket, Trp225 and Arg242, for further investigations (Figs. 5B and 6A).

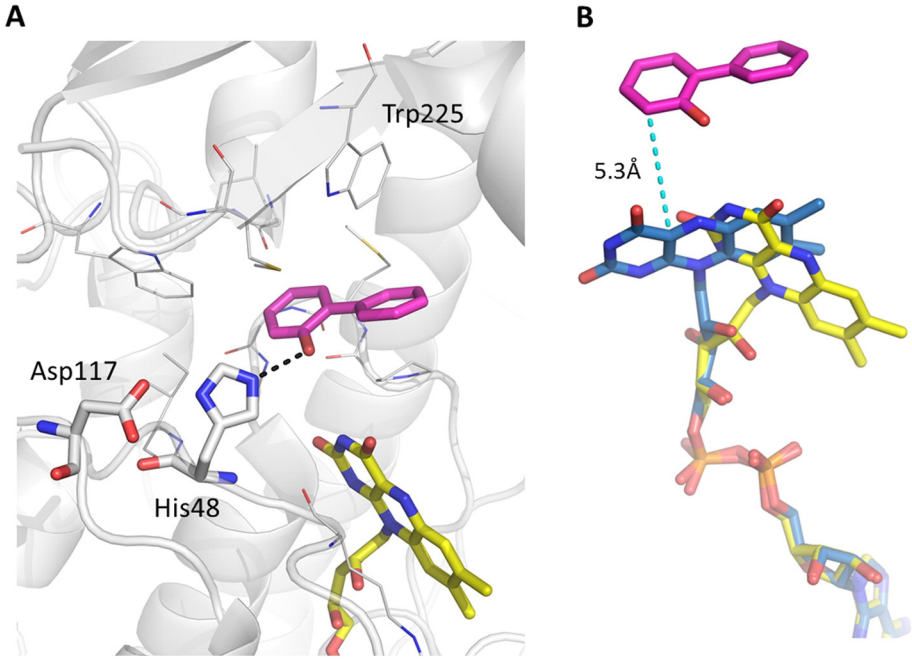

Fig. 6. 2-hydroxybiphenyl bound in the active site of HbpA. A. 2-Hydroxybiphenyl (magenta) is located in the hydrophobic pocket of HbpA (gray lines) above the FAD (yellow sticks) and forms a hydrogen bond (black dashed lines) with His48 (gray sticks), B. Superposition of FAD binding site of HbpA-HBP (yellow) with HbpA-IN (PDB code 4CY8, blue) shows that the *ortho* position of 2-hydroxybiphenyl (magenta) is located 5.3 Å (cyan dashed line) above the C4 of the isoalloxazine ring in the "in" conformation (PDB code 4CY8, blue).

Trp225 is located at the tunnel which directs the substrate into the active site. This residue is averagely conserved among flavin monooxygenases (http://consurf.tau.ac.il/). In RdmE and pHBH, this position is occupied with Tyr224 and Tyr201 respectively (Fig. 7) [12,38]. Mutating Tyr224 to Phe in RdmE resulted in an inactive enzyme, while mutating Tyr201 to Phe in pHBH resulted in a 10-fold decrease in activity and loss in substrate hydroxylation capacity [14,19,41]. Structure–function studies of pHBH suggested that Tyr201 activates the substrate for hydroxylation [19,41,42]. In order to elucidate the role of Trp225 in HbpA, we replaced Trp with Ala and Tyr. While variant W225Y showed elevated specific activity and similar hydroxylation efficiency, variant W225A exhibited a 14-fold decrease in specific activity and 7-fold decrease in hydroxylation efficiency (Table 1). Variants W225Y and W225A demonstrated a 7-fold and 9-fold decrease in *K*m values, respectively, suggesting decreased affinity towards the substrate (Table 2). The increased product formation by variant W225Y may be explained by the increased efficiency towards NADH oxidation (Table 1). We determined the crystal structure of variant W225Y (Table S2, Fig. S2). The overall structure of W225Y was similar to the structure of the wild type enzyme, suggesting that the elevated activity of variant W225Y is due solely to the Tyr residue at position 225 and not as a result of structural conformational changes which occurred due to the mutagenesis. Since Tyr at position 225 increased the efficiency towards NADH oxidation by 3-fold, we suggest that position 225 might be indirectly involved with NADH binding or oxidation by inducing local conformational changes during NADH binding. We propose that the function of Trp225 in HbpA is to properly orient 2-hydroxybiphenyl while entering the active site by forming π–π interactions thus promoting its hydroxylation (Fig. 5B). By replacing a bulky Trp with Ala, aromatic ring stacking interactions were abolished, affecting substrate orientation in the active site and decreasing enzymatic activity.

In contrast to Trp225, Arg242 is a conserved residue, located above the isoalloxazine ring of FAD forming a polar interaction with O4 of the FAD molecule in the "out" conformation (Fig. 4B and C). Replacing the corresponding residue to Gln in pHBH resulted in a 100-fold activity decrease and conformational changes of the substrate binding domain [13]. In addition, it was proposed that the role of this Arg residue is to modulate the movement of the FAD molecule. In order to investigate the role of Arg242 in HbpA, we mutated it to Ala, Gln and Glu. For all three variants, low NADH consumption was measured while no product formation was observed by HPLC analysis after 30 min (Table 1). It should be noted that Jensen et al. reported a 15% substrate conversion after 2 h for variant R242A [27]. In addition, in the present study, all three variants exhibited very low efficiency for NADH, about 20- to 60-fold decrease (Table 2). We determined the crystal structure of variant R242Q (Table S2, Fig. S2), however in contrast to pHBH, there were no changes in the structural conformation due to the replacement of Arg242 with Gln, and the FAD molecule was found in the "out" conformation, similar to its position in wild type HbpA [13]. We conclude that Arg242 is pivotal for enabling the movement of the FAD molecule. Perhaps due to the local environmental changes during substrate binding and deprotonation, this residue changes its conformation to stabilize the "out" conformation of the isoalloxazine ring, thus enabling FAD reduction by NADH. Since the replacement of Arg242 with Ala, Gln or Glu resulted in activity and especially hydroxylation capacity loss, it seems that the demand for Arg in position 242 is due to the unique architecture of the HbpA active site.

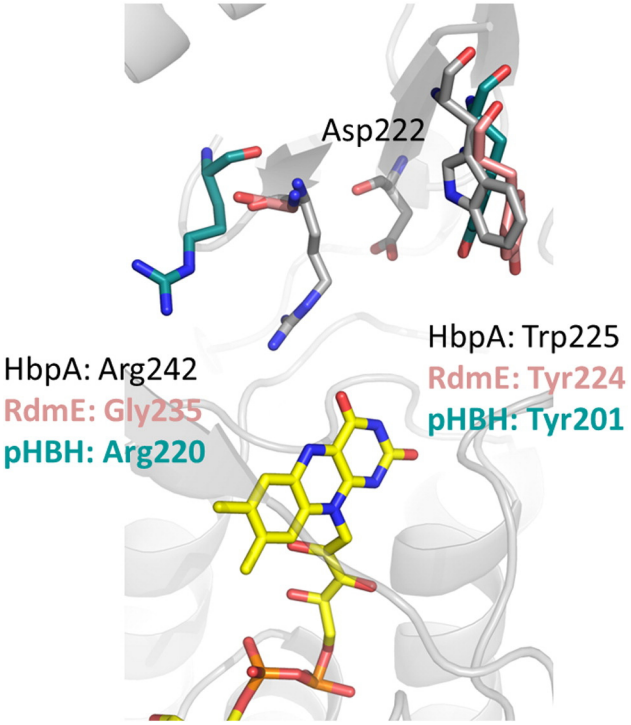

Fig. 7. Active site of HbpA. The active site of HbpA was superimposed with RdmE and pHBH (PDB codes 3IHG and 1IUV, respectively). Arg242, Asp222 and Trp225 in HbpA are shown as gray sticks. Corresponding residues to Asp242 and Trp225 in RdmE and pHBH are presented as pink and ivory sticks, respectively.

Previous investigations of HbpA suggested that Asp222, located in the binding site, plays a role in substrate activation (Figs. 6 and 7). Meyer et al. showed that the replacement of Asp222 with Val enabled indole hydroxylation but decreased the hydroxylation of 2-hydroxybiphenyl to 2,3-dihydroxybiphenyl [22]. Using a structural model of HbpA it was proposed that Asp222 is situated in the homologous position to Tyr201 in pHBH, thus similarly to Tyr201, it activates the substrate. However, the high resolution crystal structure of HbpA revealed that Trp225 and not Asp222 in HbpA is situated in a corresponding position to Tyr201 in pHBH. In addition, the fact that mutating Asp222 to Val did not drastically decrease protein activity as in the case of pHBH, suggests that Asp222 is not involved in substrate activation but perhaps in substrate orientation in the binding site.

4. Conclusion

HbpA, a flavin-dependent monooxygenase belonging to group A, was previously shown to hydroxylate numerous aromatic substrates at the *ortho* position. Although it shares a similar fold with formerly investigated flavin monooxygenases, a different binding site architecture results in a different substrate binding mode and a unique way of catalysis in terms of participating amino acids. In this work, we presented a structure of HbpA with 2-hydroxybiphenyl in the active site. The orientation of the substrate, along with the observed hydrogen bond between the substrate and His48, confirmed the previously suggested role of this residue in substrate deprotonation [27]. We suggest that Arg242 in HbpA is central in facilitating FAD movement and reduction, while residue Trp293 orients FAD in the "out" conformation and isolates it from the environment when FAD is found in the "in" conformation. Trp225 helps to appropriately orient the entering substrate into correct positioning within the binding site. In addition, biochemical investigations of variant G255F revealed that a bulky Phe at position 255 hindered substrate entrance into the active site and affected NADH binding or oxidation. To conclude, high resolution crystal structures of HbpA and site specific mutants provided a better understanding of the enzymatic mechanism and will further aid in protein engineering of biocatalysts with potential industrial applications.

Transparency Document

The Transparency Document associated with this article can be found in the online version.

Acknowledgments

This research benefited from the use of the Technion Center of Structural Biology facility of the Lorry I. Lokey Center for Life Sciences and Engineering, and the Russell Berrie Nanotechnology Institute. We thank Dr. Hay Dvir from the Technion Center of Structural Biology facility for assistance in diffraction data collection. We also thank the staff of the European Synchrotron Radiation Facility in France, beamlines ID14-4 and BM-14 for provision of synchrotron radiation facilities and assistance. The support of COST Action CM1303-Systems Biocatalysis is greatly acknowledged.

Appendix A. Supplementary data

Supplementary data to this article can be found online at http://dx.doi.org/10.1016/j.bbapap.2015.08.002.

References

[1] H.P. Kohler, D. Kohler-Staub, D.D. Focht, Degradation of 2-hydroxybiphenyl and 2,2′-dihydroxybiphenyl by *Pseudomonas sp.* strain HBP1, Appl. Environ. Microbiol. 54 (1988) 2683–2688.
[2] W.A. Suske, M. Held, A. Schmid, T. Fleischmann, M.G. Wubbolts, H.P. Kohler, Purification and characterization of 2-hydroxybiphenyl 3-monooxygenase, a novel NADH-dependent, FAD-containing aromatic hydroxylase from *Pseudomonas azelaica* HBP1, J. Biol. Chem. 272 (1997) 24257–24265.
[3] M.M.E. Huijbers, S. Montersino, A.H. Westphal, D. Tischler, W.J.H. van Berkel, Flavin dependent monooxygenases, Arch. Biochem. Biophys. 544 (2014) 2–17.
[4] A. Meyer, A. Schmid, M. Held, A.H. Westphal, M. Rothlisberger, H.P. Kohler, W.J.H. van Berkel, B. Witholt, Changing the substrate reactivity of 2-hydroxybiphenyl 3-monooxygenase from *Pseudomonas azelaica* HBP1 by directed evolution, J. Biol. Chem. 277 (2002) 5575–5582.
[5] F. Hollmann, A. Schmid, E. Steckhan, The first synthetic application of a monooxygenase employing indirect electrochemical NADH regeneration, Angew. Chem. Int. Ed. 40 (2001) 169–171.
[6] M. Held, W. Suske, A. Schmid, K.-H. Engesser, H.-P.E. Kohler, B. Witholt, M.G. Wubbolts, Preparative scale production of 3-substituted catechols using a novel monooxygenase from *Pseudomonas azelaica* HBP 1, J. Mol. Catal. B Enzym. 5 (1998) 87–93.
[7] C.N. Jensen, J. Cartwright, J. Ward, S. Hart, J.P. Turkenburg, S.T. Ali, M.J. Allen, G. Grogan, A flavoprotein monooxygenase that catalyses a Baeyer-Villiger reaction and thioether oxidation using NADH as the nicotinamide cofactor, ChemBioChem 13 (2012) 872–878.
[8] M.H.M. Eppink, W.J.H. van Berkel, H.A. Schreuder, Identification of a novel conserved sequence motif in flavoprotein hydroxylases with a putative dual function in FAD/NAD(P)H binding, Protein Sci. 6 (1997) 2454–2458.
[9] C. Laane, W.J. van Berkela, Flavoenzyme-catalyzed oxygenations and oxidations of phenolic compounds, Adv. Synth. Catal. 344 (2002) 1023–1035.
[10] W.J.H. van Berkel, N.M. Kamerbeek, M.W. Fraaije, Flavoprotein monooxygenases, a diverse class of oxidative biocatalysts, J. Biotechnol. 124 (2006) 670–689.
[11] W.A. Suske, W.J.H. van Berkel, H.-P.E. Kohler, Catalytic mechanism of 2-hydroxybiphenyl 3-monooxygenase, a flavoprotein from *Pseudomonas azelaica* HBP1, J. Biol. Chem. 274 (1999) 33355–33365.
[12] H.A. Schreuder, P.A. Prick, R.K. Wierenga, G. Vriend, K.S. Wilson, W.G. Hol, J. Drenth, Crystal structure of the *p*-hydroxybenzoate hydroxylase-substrate complex refined at 1.9 Å resolution: analysis of the enzyme-substrate and enzyme-product complexes, J. Mol. Biol. 208 (1989) 679–696.
[13] J. Wang, M. Ortiz-Maldonado, B. Entsch, V. Massey, D. Ballou, D.L. Gatti, Protein and ligand dynamics in 4-hydroxybenzoate hydroxylase, Proc. Natl. Acad. Sci. U. S. A. 99 (2002) 608–613.
[14] D. Gatti, B. Palfey, M. Lah, B. Entsch, V. Massey, D. Ballou, M. Ludwig, The mobile flavin of 4-OH benzoate hydroxylase, Science 266 (1994) 110–114.
[15] C. Enroth, H. Neujahr, G. Schneider, Y. Lindqvist, The crystal structure of phenol hydroxylase in complex with FAD and phenol provides evidence for a concerted conformational change in the enzyme and its cofactor during catalysis, Structure 6 (1998) 605–617.
[16] H.A. Schreuder, A. Mattevi, G. Obmolova, K.H. Kalk, W.G.J. Hol, F.J.T. van der Bolt, W.J.H. van Berkel, Crystal structures of wild-type p-hydroxybenzoate hydroxylase complexed with 4-aminobenzoate, 2,4-dihydroxybenzoate, and 2-hydroxy-4-aminobenzoate and of the tyr222ala mutant complexed with 2-hydroxy-4-aminobenzoate. Evidence for a proton channel and a new binding mode of the flavin ring, Biochemistry 33 (1994) 10161–10170.
[17] W.J.H. van Berkel, M.H. Eppink, H.A. Schreuder, Crystal structure of p-hydroxybenzoate hydroxylase reconstituted with the modified FAD present in alcohol oxidase from methylotrophic yeasts: evidence for an arabinoflavin, Protein Sci. 3 (1994) 2245–2253.
[18] B. Entsch, L.J. Cole, D.P. Ballou, Protein dynamics and electrostatics in the function of p-hydroxybenzoate hydroxylase, Arch. Biochem. Biophys. 433 (2005) 297–311.
[19] B. Entsch, B.A. Palfey, D.P. Ballou, V. Massey, Catalytic function of tyrosine residues in para-hydroxybenzoate hydroxylase as determined by the study of site-directed mutants, J. Biol. Chem. 266 (1991) 17341–17349.
[20] T. Hiromoto, S. Fujiwara, K. Hosokawa, H. Yamaguchi, Crystal structure of 3-hydroxybenzoate hydroxylase from *Comamonas testosteroni* has a large tunnel for substrate and oxygen access to the active site, J. Mol. Biol. 364 (2006) 878–896.
[21] B. Tomaszewski, A. Schmid, K. Buehler, Biocatalytic production of catechols using a high pressure tube-in-tube segmented flow microreactor, Org. Process Res. Dev. 18 (2014) 1516–1526.
[22] A. Meyer, M. Würsten, A. Schmid, H.P. Kohler, B. Witholt, Hydroxylation of indole by laboratory-evolved 2-hydroxybiphenyl 3-monooxygenase, J. Biol. Chem. 277 (2002) 34161–34167.
[23] J. Lutz, F. Hollmann, T.V. Ho, A. Schnyder, R.H. Fish, A. Schmid, Bioorganometallic chemistry: biocatalytic oxidation reactions with biomimetic NAD+/NADH cofactors and [Cp*Rh(bpy)H] + for selective organic synthesis, J. Organomet. Chem. 689 (2004) 4783–4790.
[24] J. Lutz, V.V. Mozhaev, Y.L. Khmelnitsky, B. Witholt, A. Schmid, Preparative application of 2-hydroxybiphenyl 3-monooxygenase with enzymatic cofactor regeneration in organic-aqueous reaction media, J. Mol. Catal. B Enzym. 19–20 (2002) 177–187.
[25] A. Schmid, I. Vereyken, M. Held, B. Witholt, Preparative regio- and chemoselective functionalization of hydrocarbons catalyzed by cell free preparations of 2-hydroxybiphenyl 3-monooxygenase, J. Mol. Catal. B Enzym. 11 (2001) 455–462.
[26] V. Köhler, Y. Wilson, M. Dürrenberger, D. Ghislieri, E. Churakova, T. Quinto, L. Knörr, D. Häussinger, F. Hollmann, N. Turner, Synthetic cascades are enabled by combining biocatalysts with artificial metalloenzymes, Nat. Chem. 5 (2013) 93–99.
[27] C.N. Jensen, T. Mielke, J.E. Farrugia, A. Frank, H. Man, S. Hart, J.P. Turkenburg, G. Grogan, Structures of the apo and FAD-bound forms of 2-hydroxybiphenyl 3-monooxygenase (HbpA) locate activity hotspots identified by using directed evolution, ChemBioChem 16 (2015) 968–976.
[28] S. Lansky, O. Alalouf, V. Solomon, A. Alhassid, L. Govada, N.E. Chayan, H. Belrhali, Y. Shoham, G. Shoham, Crystallization and preliminary crystallographic analysis of Axe2, an acetylxylan esterase from *Geobacillus stearothermophilus*, Acta Crystallogr. Sect. F 69 (2013) 430–434.
[29] M. Goldfeder, M. Kanteev, S. Isaschar-Ovdat, N. Adir, A. Fishman, Determination of tyrosinase substrate-binding modes reveals mechanistic differences between type-3 copper proteins, Nat. Commun., vol. 5, Nature Publishing Group, a division of Macmillan Publishers Limited, 2014 (All Rights Reserved).
[30] A. Leslie, Availability of the MOSFLM program suite for processing image plate and film data, in: W.M. Wolf, K.S. Wilson (Eds.),Joint CCP4 and ESF-EACBM Newsletter on Protein Crystallography, 1992.
[31] Z. Otwinowski, W. Minor, DENZO and SCALEPACK, in: M.G. Rossmann, E. Arnold (Eds.), International Tables for Crystallography Volume F: Crystallography of Biological Macromolecules volume FSpringer Netherlands 2001, pp. 226–235.
[32] P.D. Adams, P.V. Afonine, G. Bunkóczi, V.B. Chen, I.W. Davis, N. Echols, J.J. Headd, L.-W. Hung, G.J. Kapral, R.W. Grosse-Kunstleve, A.J. McCoy, N.W. Moriarty, R. Oeffner, R.J. Read, D.C. Richardson, J.S. Richardson, T.C. Terwilliger, P.H. Zwart, PHENIX: a comprehensive Python-based system for macromolecular structure solution, Acta Crystallogr. Sect. D 66 (2010) 213–221.
[33] A. McCoy, Solving structures of protein complexes by molecular replacement with Phaser, Acta Crystallogr. Sect. D 63 (2007) 32–41.
[34] P. Emsley, K. Cowtan, Coot: model-building tools for molecular graphics, Acta Crystallogr. Sect. D 60 (2004) 2126–2132.
[35] S. Bisagni, R. Hatti-Kaul, G. Mamo, Cloning, expression and characterization of a versatile Baeyer-Villiger monooxygenase from *Dietzia* sp. D5, Appl. Microbiol. Biotechnol. Express 4 (2014) 1–10.
[36] C.A. Bottoms, P.E. Smith, J.J. Tanner, A structurally conserved water molecule in Rossmann dinucleotide-binding domains, Protein Sci. 11 (2002) 2125–2137.
[37] J.L. Martin, Thioredoxin — a fold for all reasons, Structure 3 (1995) 245–250.
[38] Y. Lindqvist, H. Koskiniemi, A. Jansson, T. Sandalova, R. Schnell, Z. Liu, P. Mantsala, J. Niemi, G. Schneider, Structural basis for substrate recognition and specificity in aklavinone-11-hydroxylase from rhodomycin biosynthesis, J. Mol. Biol. 393 (2009) 966–977.
[39] K.S. Ryan, A.R. Howard-Jones, M.J. Hamill, S.J. Elliott, C.T. Walsh, C.L. Drennan, Crystallographic trapping in the rebeccamycin biosynthetic enzyme RebC, Proc. Natl. Acad. Sci. U. S. A. 104 (2007) 15311–15316.
[40] S. Montersino, R. Orru, A. Barendregt, A.H. Westphal, E. van Duijn, A. Mattevi, W.J.H. van Berkel, Crystal structure of 3-hydroxybenzoate 6-hydroxylase uncovers lipid-assisted flavoprotein strategy for regioselective aromatic hydroxylation, J. Biol. Chem. 288 (2013) 26235–26245.
[41] K. Eschrich, F.J.T. van der Bolt, A. de Kok, W.J.H. van Berkel, Role of Tyr201 and Tyr385 in substrate activation by p-hydroxybenzoate hydroxylase from *Pseudomonas fluorescens*, Eur. J. Biochem. 216 (1993) 137–146.
[42] D.L. Gatti, B. Entsch, D.P. Ballou, M.L. Ludwig, pH-dependent structural changes in the active site of p-hydroxybenzoate hydroxylase point to the importance of proton and water movements during catalysis, Biochemistry 35 (1996) 567–578.